

The role of pressure gradients in driving sunward magnetosheath flows and magnetopause motion

M. O. Archer,¹

D. L. Turner,²

J. P. Eastwood,¹

T. S. Horbury,¹

and S. J. Schwartz¹

M. O. Archer, Space & Atmospheric Physics Group, The Blackett Laboratory, Imperial College London, Prince Consort Road, London, SW7 2AZ, UK. (m.archer10@imperial.ac.uk)

D. L. Turner, Department of Earth, Planetary and Space Sciences, University of California, 603 Charles E. Young Drive, Los Angeles, California, CA 90095-1567, USA. (dturner@igpp.ucla.edu)

J. P. Eastwood, Space & Atmospheric Physics Group, The Blackett Laboratory, Imperial College London, Prince Consort Road, London, SW7 2AZ, UK. (jonathan.eastwood@imperial.ac.uk)

T. S. Horbury, Space & Atmospheric Physics Group, The Blackett Laboratory, Imperial College London, Prince Consort Road, London, SW7 2AZ, UK. (t.horbury@imperial.ac.uk)

S. J. Schwartz, Space & Atmospheric Physics Group, The Blackett Laboratory, Imperial College London, Prince Consort Road, London, SW7 2AZ, UK. (s.schwartz@imperial.ac.uk)

¹Blackett Laboratory, Imperial College
London, London, SW7 2AZ, UK.

Abstract. While pressure balance can predict how far the magnetopause will move in response to an upstream pressure change, it cannot determine how fast the transient reponse will be. Using Time History of Events and Macroscale Interactions during Substorms (THEMIS), we present multipoint observations revealing, for the first time, strong (thermal + magnetic) pressure gradients in the magnetosheath due to a foreshock transient, most likely a Hot Flow Anomaly (HFA), which decreased the total pressure upstream of the bow shock. By converting the spacecraft time series into a spatial picture, we quantitatively show that these pressure gradients caused the observed acceleration of the plasma, resulting in fast sunward magnetosheath flows ahead of a localised outward distortion of the magnetopause. The acceleration of the magnetosheath plasma was fast enough to keep the peak of the magnetopause bulge at approximately the equilibrium position i.e. in pressure balance. Therefore, we show that pressure gradients in the magnetosheath due to transient changes in the total pressure upstream can directly drive anomalous flows and in turn are important in transmitting information from the bow shock to the magnetopause.

²Department of Earth, Planetary and
Space Sciences, University of California, Los
Angeles, California, CA 90095-1567, USA.

1. Introduction

The location of the magnetopause in equilibrium is given by a balance of pressure between the solar wind and magnetosphere, with the shocked magnetosheath forming an interface between the two. However, while pressure balance can determine how far the magnetopause should move in response to changes in the pressure upstream of the bow shock, it cannot predict how fast this motion will occur. *Glassmeier et al.* [2008] showed that if the magnetosheath pressure changes over long enough ($\sim 5\text{--}7$ min) timescales then the response of the magnetopause can be treated quasistatically. In contrast, the solar wind dynamic pressure can rapidly change due to, for example, tangential discontinuities (TDs) exhibiting step changes in the density and thus dynamic pressure. 1-D magnetohydrodynamic (MHD) simulations [Völk and Auer, 1974; Wu et al., 1993] of the bow shock's response to such dynamic pressure drops predict that the shock will move sunward and that a fast mode rarefaction wave will propagate through the magnetosheath ahead of the transmitted TD. This fast mode wave will exhibit a (thermal + magnetic) pressure gradient across it which should weaken in time as the wave front expands. Eventually arriving at the magnetopause, the wave communicates the upstream pressure change to the boundary, which will subsequently move in response. These waves have been observed due to such solar wind dynamic pressure decreases [Maynard et al., 2007], however the magnetosheath pressure gradients and how these affect the magnetosheath plasma and in turn the magnetopause have not yet been measured due to a lack of suitable multipoint observations in the magnetosheath.

Wu et al. [1993] predicted that if the decrease in dynamic pressure is sufficiently large, then the magnetosheath may experience a sunward flow due to the rarefaction behind the rapidly expanding bow shock. While anomalous sunward flows have previously been observed in the magnetosheath [e.g. *Paschmann et al.*, 1988; *Schwartz et al.*, 1988; *Thomsen et al.*, 1988; *Shue et al.*, 2009], their origins in general have been unclear due to a lack of simultaneous observations upstream of the shock. It is possible that foreshock transients may play an important role regarding anomalous magnetosheath flows, since they too can modify the total pressure upstream. They are kinetic phenomena which occur due to the ever changing orientation of the interplanetary magnetic field (IMF) and solar wind conditions, thereby changing the location and properties of the foreshock [e.g. *Eastwood et al.*, 2005].

A number of different types of foreshock transients have been identified in both spacecraft observations and simulations including: hot flow anomalies (HFAs) [e.g. *Schwartz et al.*, 1985] caused by the interaction of solar wind current sheets with the bow shock; spontaneous hot flow anomalies, phenomenologically similar to HFAs but without the need for a solar wind current sheet [e.g. *Zhang et al.*, 2013; *Omidi et al.*, 2013a]; foreshock cavities [e.g. *Sibeck et al.*, 2002] caused due to an isolated collection of field lines connected to the quasi-parallel bow shock; and foreshock bubbles [*Omidi et al.*, 2010; *Turner et al.*, 2013] due to the interaction of backstreaming suprathermal ions with a discontinuity. These foreshock transients are important because they can perturb the magnetopause boundary, generating ultra-low frequency waves in the magnetosphere and travelling convection vortices in the ionosphere [*Sibeck et al.*, 1999; *Eastwood et al.*, 2008, 2011; *Jacobsen et al.*, 2009; *Turner et al.*, 2011; *Hartinger et al.*, 2013].

HFAs in particular are disruptions of the solar wind in the vicinity of the bow shock caused by current sheets, usually TDs, interacting with the shock [e.g. *Wang et al.*, 2013a, b]. If the solar wind motional electric field $\mathbf{E} = -\mathbf{v} \times \mathbf{B}$ points into the TD on at least one side, ions specularly reflected at the shock are channeled back along the current sheet [*Burgess*, 1989; *Thomas et al.*, 1991]. The resulting hot ion population expands forming a core region of depleted density and magnetic field and laterally drives pile up regions and shock waves either side [*Fuselier et al.*, 1987; *Lucek et al.*, 2004].

Sibeck et al. [1999] presented observations of a sunward plasma velocity at the flank magnetopause boundary, which was distorted from its usual shape into an outward bulge due to an HFA that was simultaneously observed upstream of the shock. In contrast, *Jacobsen et al.* [2009] showed that HFAs in the flanks can deform the magnetopause inwards and cause fast anomalous flows. The authors explain these observations as being due to the reduced (increased) total pressure in the HFA core (compression) regions being transmitted through the magnetosheath and thus the magnetopause moving in order to balance the pressure. This is broadly in agreement with the suggestions from simulations of HFAs [*Lin*, 2002; *Omidi and Sibeck*, 2007], which also predict marginally sunward flows in the magnetosheath due to the presence of the HFA. Nonetheless, the mechanism by which upstream pressure variations due to foreshock transients are transmitted through the bow shock and magnetosheath to the magnetopause are poorly understood.

In this paper we determine the pressure gradient in the magnetosheath for the first time using multipoint observations, quantitatively showing that these gradients directly drive the acceleration of the plasma resulting in fast sunward flows and causing the subsequent motion of the magnetopause. Through simultaneous observations upstream of the bow

shock we show that the observed gradients in the magnetosheath were due to a foreshock transient, most likely an HFA, which reduced the upstream total pressure.

2. Observations

2.1. Magnetosheath & Magnetopause Observations

On 04 September 2008 between 17:32-42 UT, three of the THEMIS [Angelopoulos, 2008] spacecraft (THD, THE and THA) were located in the subsolar magnetosheath separated by $\sim 1 R_E$ (see Figure 1). Combined Electrostatic Analyzer (ESA) [McFadden *et al.*, 2008a] and Solid State Telescope (SST) moments and energy spectrograms are displayed in Figure 2, revealing a transient change in the magnetosheath ion velocity at all three spacecraft from the regular $\sim 100 \text{ km s}^{-1}$ flow in an anti-sunward direction to enhanced magnetosheath flows travelling sunwards (blue shaded regions). The sunward component of the velocity was fastest ($\sim 230 \text{ km s}^{-1}$) and longest ($\sim 2^{3/4} \text{ min}$) at THD, furthest from Earth, whereas it was slowest ($\sim 120 \text{ km s}^{-1}$) and shortest ($\sim 40 \text{ s}$) at THA, closest to Earth. Following the sunward flows, the magnetopause passed over all three spacecraft, which subsequently had brief excursions in the magnetosphere, before encountering the boundary again and returning to the magnetosheath. The relative magnetopause crossing times (vertical dashed lines in Figure 2) were, however, inconsistent with a global “breathing” motion of the boundary, which would result in nested crossings due to the spacecraft’s geocentric distances.

We used minimum variance analysis (MVA) [e.g. Sonnerup and Scheible, 1998] of the spin-resolution Fluxgate Magnetometer (FGM) data [Auster *et al.*, 2008] to determine normals for the observed magnetopause crossings, testing the quality of the analysis via the intermediate-to-minimum eigenvalue ratio test ($\lambda_{int}/\lambda_{min} \gtrsim 10$ implying a reliable

normal) as well as the sensitivity of the resulting normal to different time intervals centred on the boundary. For the inbound crossings, the THD observations provided the most reliable normal $\mathbf{n} = (0.70, -0.67, -0.23)$ in GSE coordinates which is deflected, predominantly towards the -y GSE direction, by 36° from the expected orientation of the normal \mathbf{N} from the *Shue et al.* [1998] model magnetopause. For all spacecraft pairs we used the two spacecraft timing method [e.g. *Schwartz, 1998*] to estimate the magnetopause speed along the normal, yielding an average value $v_n = 122 \pm 7 \text{ km s}^{-1}$: much faster than typical motions though within the range of those previously observed [e.g. *Plaschke et al., 2009*]. The orientation of the magnetopause crossing indicates that there was a localised outwards distortion of the magnetopause moving across the model boundary. The transit velocity of this bulge \mathbf{v}_{trans} , given by [*Schwartz et al., 2000*]

$$\mathbf{v}_{trans} = \frac{v_n}{\sin^2 \theta_{Nn}} (\mathbf{n} - \cos \theta_{Nn} \mathbf{N}) \quad (1)$$

where θ_{Nn} is the angle between the two normals, was found to be $(-19, -205, 12) \text{ km s}^{-1}$ in GSE coordinates. While no reliable magnetopause normals could be obtained from MVA for the outbound crossings, we estimated the trailing edge's orientation by three spacecraft timing [*Horbury et al., 2001*] using the transit velocity of the leading edge \mathbf{v}_{trans} . This resulted in an outbound normal deflected, predominantly towards the +y GSE direction, by 29° from the model boundary. Therefore, the magnetopause was locally distorted into an outward bulge.

The bottom panels of Figure 2 show the combined isotropic ion and electron thermal pressure P_{th} , the magnetic pressure P_B and the anti-sunward dynamic pressure $P_{dyn,x}$ (for only those intervals in which the flow was antisunward) as well as the sum of these,

the total pressure $P_{tot,x}$. All spacecraft observed a decrease in the total pressure (from the background value of ~ 2 nPa) during the event, first observed at THD and followed ~ 55 s later by THA and THE in quick succession. This decrease was greatest (~ 1.2 nPa) at THD and only marginal (~ 0.3 nPa) at THA. Therefore there was a pressure gradient through the magnetosheath, driving the sunward flows and outward magnetopause motion as we show in section 3. Next we investigate the origin of this pressure gradient through observations upstream of the bow shock.

2.2. Solar Wind & Foreshock Observations

Figure 3 shows simultaneous observations upstream of the bow shock from THB (red) and THC (green) along with Magnetic Field Investigation data [Lepping *et al.*, 1995] from the WIND spacecraft (black) near L1, which has been lagged by 32 min (plasma data is not shown due to its low time resolution of 97 s which revealed no strong variations). The time lag was obtained by matching up the magnetic field signatures between WIND and the THEMIS spacecraft. We highlight (grey areas) two directional discontinuities, denoted DD1 and DD2, between which the IMF was radial and backstreaming suprathermal ions (see ion spectrograms) typical of the ion foreshock [e.g. Eastwood *et al.*, 2005] were observed. These suprathermal populations caused the observed increases in parallel ion temperature moments (over the entire distributions) during this period.

On the downstream edge of DD2, a region of depleted density and magnetic field was observed by both THEMIS spacecraft (yellow area) with compressions either side. These correlated variations, which were not present in the almost steady pristine solar wind, are indicative of foreshock transients [Fairfield *et al.*, 1990]. Within the depleted core, “3 s waves” [Le *et al.*, 1992] (almost circularly polarised waves that are right-handed in

the spacecraft frame) were observed which typically occur in the foreshock under high solar wind plasma β conditions ($\beta \sim 5$ here); the solar wind was slowed; and the ion temperatures moments (over the entire distributions) marginally increased both parallel and perpendicular to the magnetic field. In addition the ion distributions (not shown) were more diffuse compared to the intermediate distributions observed outside of this region, though the solar wind beam persisted throughout. Note that these variations were observed simultaneously at both THEMIS spacecraft but were all larger at THC, closer to the bow shock.

Since MVA was poorly conditioned ($\lambda_{int}/\lambda_{min} \sim 1$), we determined the orientation of DD2 using a constrained two spacecraft timing method between THB and WIND. The normal \mathbf{n}_{DD2} was constructed using the regular two spacecraft timing method ($\{\mathbf{r}_{\alpha\beta} - \mathbf{v}_{sw}t_{\alpha\beta}\} \cdot \mathbf{n}_{DD2} = 0$ where $\mathbf{r}_{\alpha\beta}$ is the spacecraft separation vector and $t_{\alpha\beta}$ the relative timing between the spacecraft) and by requiring it be perpendicular to the maximum variance direction ($\mathbf{e}_{max} \cdot \mathbf{n}_{DD2} = 0$), which was better defined than the minimum ($\lambda_{max}/\lambda_{int} \sim 24$). The computed normal was found to be almost entirely in the GSE y direction: (0.09,0.99,0.10) in GSE coordinates. This was close (within $\sim 12^\circ$) to the theoretical normal for a TD given by the cross product of the upstream and downstream magnetic fields [e.g. *Knetter et al.*, 2004].

Considering the thermal, magnetic and dynamic pressures upstream of the shock (bottom panel of Figure 3), it was found that the total pressure associated with the core of this transient was dominated by the dynamic pressure and this varied chiefly due to the density changes rather than the velocity. The total pressure at THC, closest to the bow shock, decreased (from its ambient value of ~ 2.0 nPa) by ~ 1.4 nPa in the depleted core,

with increases of ~ 0.3 nPa and ~ 0.7 nPa before and after respectively; thus the total pressure upstream of the bow shock was modified due to the presence of the transient.

This foreshock transient cannot be explained as a Foreshock Bubble since it satisfies none of the *Turner et al.* [2013] criteria for Foreshock Bubble identification. This transient could be a Foreshock Cavity, since there was a localised region of plasma connected to the quasi-parallel shock [*Schwartz et al.*, 2006] between DD1 and DD2. However, the transient formed at DD2 (most clear at THB) rather than filling the space between the two discontinuities, unlike a typical Foreshock Cavity. In contrast, the event did satisfy all the *Schwartz et al.* [2000] conditions for HFA identification: the electric field pointed into the current sheet on the upstream side and the discontinuity normal was almost perpendicular to the Sun-Earth line. In addition there was very little change in the magnetic field strength across the discontinuity and quasi-perpendicular bow shock conditions were present on the upstream side, which are typical for HFAs [*Schwartz et al.*, 2000]. Further evidence towards an HFA include the depleted core being displaced towards the side of the discontinuity magnetically connected to the quasi-parallel bow shock [*Omidí and Sibeck*, 2007; *Zhang et al.*, 2010; *Wang et al.*, 2013b]; the existence of compressions either side of this core region [e.g. *Schwartz et al.*, 1988]; and the differences between the two THEMIS spacecraft, showing simultaneously weaker variations further upstream, in agreement with the locality of HFAs to the bow shock. However, the plasma moments showed no large deflections in the ion velocity nor significant heating of the thermal ion plasma, the typical signatures of an HFA. The observations were very similar to the “proto-HFA” presented by *Zhang et al.* [2010], in which simultaneous observations closer to the bow shock revealed stronger HFA signatures including significant heating and shocks i.e.

the signatures of the “proto-HFA” were observations taken further upstream of an HFA at the bow shock. On the other hand, *Omidi et al.* [2013b] have shown through 2-D kinetic hybrid simulations that a succession of two discontinuities resulting in a localised foreshock between them, similar to the case here, can lead to somewhat similar correlated density and magnetic field variations. While we conclude this foreshock transient was most likely an HFA (and will refer to it as such henceforth), we cannot unambiguously determine so. Nonetheless, it is the fact that the pressure upstream of the bow shock was altered by the transient which is important here, not its specific nature.

3. Analysis

To determine whether the HFA was the cause of the sunward flows and magnetopause motions, we piece together the observations from all five THEMIS spacecraft. We assume that both the observed HFA and magnetopause disturbance time series were due to the structures simply passing over the spacecraft and not intrinsically temporal variations. This assumption leads to a consistent framework for this event, except for immediately preceding the pressure reduction where the observed density enhancements varied significantly between spacecraft meaning that there was substructure in either space or time. It is possible to turn the observed time series into the spatial picture shown in Figure 4, a snapshot of the event in the GSE frame at 17:37 UT. Since the spacecraft separation vectors, observed motions and estimated normals all have relatively small components in the GSE z direction, we can limit our spatial picture to the GSE x - y plane for simplicity. For the shape of the magnetopause (solid black line), we combine the *Shue et al.* [1998] model boundary (dotted black line) with the determined outward bulge. Using the transit velocity of the bulge \mathbf{v}_{trans} , we arrive at the spatial variations in the (thermal + magnetic)

pressure and velocity fields in the magnetosheath along the spacecraft tracks. In the case of the pressure, this has been interpolated between the three spacecraft tracks yielding the pressure contours shown in Figure 4.

DD2 (green) is indicated upstream of the *Farris et al.* [1991] model bow shock (black dashed line), showing good agreement between the intersection of the (assumed planar) current sheet with the model shock and the peak location of the outward bulge of the magnetopause. By using the total pressure observed in the HFA core from THC, we estimate through pressure balance that the magnetopause should have locally moved out to a GSE x location of $11.3 R_E$ in the plane displayed in Figure 4, which agrees well with the intersection of the (assumed planar) leading and trailing edges of the boundary disturbance at $11.5 R_E$.

Figure 4 shows a region of reduced (thermal + magnetic) pressure in the magnetosheath, spanning $\sim 4 R_E$ transverse to the bow shock, ahead of the leading edge of the magnetopause bulge. This was due to the presence of the HFA upstream of the bow shock, in particular its depleted core on the downstream edge of DD2 with decreased total pressure. The existence of a localised region of reduced pressure means that there were substantial pressure gradients in the magnetosheath. We wish to determine quantitatively whether these gradients can account for the observed accelerations of the magnetosheath flow to a sunward direction. We calculate the local (Eulerian) acceleration $\partial \mathbf{v} / \partial t$ observed by the THEMIS spacecraft from a linear fit to the velocity time series (periods indicated by the horizontal blue bars at the top of Figure 2) and then compare this to that expected from MHD theory. The MHD momentum equation (neglecting the magnetic tension force since $\beta \sim 3-8$ within the sunward flows) is given by

$$\frac{\partial \mathbf{v}}{\partial t} = -\frac{1}{\rho} \nabla (P_{th} + P_B) - \mathbf{v} \cdot \nabla \mathbf{v} \quad (2)$$

Therefore, using the pressure and velocity fields derived from the multiple spacecraft, it is possible to calculate the expected local acceleration $\partial \mathbf{v} / \partial t$ at the spacecraft locations in the GSE $z = -2.93 R_E$ plane, as shown in Figure 4. THD, furthest from Earth, observed a sunward acceleration of $(2.9, -0.1) \text{ km s}^{-2}$ in this plane. Using the right hand side of Equation 2, we arrive at an expected acceleration in this direction (primarily due to the pressure gradient since the advective term was small) of 2.7 km s^{-2} . Similarly THA, closest to Earth, observed an acceleration of $(4.6, 3.1) \text{ km s}^{-2}$, which has a magnitude of 5.5 km s^{-2} , and we compute the expected acceleration due to the pressure gradient in this direction to be 5.6 km s^{-2} . The sunward acceleration at THE varied from a value similar to that at THA to one similar to THD. The observed sunward accelerations of the magnetosheath plasma were therefore in excellent agreement with that predicted by MHD due to the determined pressure gradients. These are different at the three spacecraft due to the localised nature of the pressure decrease in the magnetosheath, meaning that the orientation of the pressure fronts (and thus the pressure gradients) are highly dependent on location, as can be seen in Figure 4.

Fast anti-sunward flows were also observed (most notably by both THE and THA) on the trailing edge of the magnetopause distortion, but again before the pressure decrease at THE. Here they are also likely due to the pressure gradient force: the total pressure upstream of the bow shock was enhanced in the HFA's compression regions and was reduced within the outward bulge of the magnetopause. Slight thermal pressure increases were observed at THE during the anti-sunwards flows ($\sim 0.8 \text{ nPa}$ and $\sim 0.5 \text{ nPa}$ respectively),

however similar increases at THA were obscured due to oscillations of the boundary. The observed jets, which enhance the total pressure on the magnetopause chiefly due to their dynamic pressure (Figure 2), could cause inward distortions of the magnetopause [e.g. *Shue et al.*, 2009] as have been observed due to HFAs previously [*Jacobsen et al.*, 2009].

4. Conclusions

We have presented a case study of fast sunward magnetosheath flows followed by motions of the magnetopause. Simultaneous observations upstream of the bow shock revealed that these were due to a foreshock transient, most likely a Hot Flow Anomaly (HFA), which had an associated decrease in total pressure. By converting the spacecraft time series into a spatial picture, we have directly shown the pressure gradients in the magnetosheath due to this pressure decrease for the first time. These pressure gradients drive the acceleration that resulted in the anomalous flow patterns, transmitting the information of the upstream pressure change through the magnetosheath to the magnetopause. In turn the boundary is no longer in pressure balance and moves, causing a localised outwards distortion of the magnetopause. Furthermore, the acceleration of the magnetosheath plasma was fast enough to keep the peak of the magnetopause bulge at approximately the equilibrium position i.e. in pressure balance.

Previous studies have shown that the reduced pressure of HFA cores can be transmitted through to the magnetosheath [*Eastwood et al.*, 2008] and subsequently cause magnetopause motions [*Sibeck et al.*, 1999; *Jacobsen et al.*, 2009] via pressure balance. Now, thanks to the geometry of the HFA and the configuration of the THEMIS spacecraft, we have shown the role of the pressure gradient force in directly driving the magnetosheath flow, with the calculated pressure gradients agreeing quantitatively with the measured

acceleration of plasma. Previous 2-D hybrid simulations of HFAs [*Lin, 2002; Omidì and Sibeck, 2007*] resulted in only very small sunward components of the magnetosheath velocity. Observations [*Eastwood et al., 2008*] have shown that not all HFAs cause sunward flows in the magnetosheath, though they do cause some flow deflections. The reason for such fast sunward flows observed here is likely due to the amplitude of the upstream pressure decrease, as per the 1-D MHD theory of *Wu et al. [1993]*. Therefore, it is important to understand the factors which control the pressure variations which develop/evolve in foreshock transients.

We have shown the role that magnetosheath pressure gradients play in transmitting information about upstream pressure variations, in this case due to a foreshock transient. However such variations can originate from other types of transients [e.g. *Sibeck et al., 2002; Omidì et al., 2010*] as well as from the solar wind [e.g. *Potemra et al., 1989*]. Whether the flow is accelerated to become sunward will depend not only on the strength of the gradients but also on the location in the magnetosheath, with sunward flows theoretically being more easily achieved close to the magnetopause due to the reduced magnetosheath velocities. Further multipoint observations in the magnetosheath could therefore allow us to better understand the pressure gradients which form due to a number of different phenomena under different conditions and the effect these have on driving anomalous magnetosheath flows and magnetopause motions.

Acknowledgments. M. O. Archer would like to thank H. Hietala for helpful discussions. This research at Imperial College London was funded by STFC grants ST/I505713/1, ST/K001051/1 and ST/G00725X/1. D. L. Turner is thankful for funding from NASA (THEMIS mission and grant NNX14AC16G). We acknowledge NASA

contract NAS5-02099 and V. Angelopoulos for use of data from the THEMIS Mission, specifically C. W. Carlson and J. P. McFadden for use of ESA data; D. Larson and R. P. Lin for use of SST data; and K. H. Glassmeier, U. Auster and W. Baumjohann for the use of FGM data provided under the lead of the Technical University of Braunschweig and with financial support through the German Ministry for Economy and Technology and the German Center for Aviation and Space (DLR) under contract 50 OC 0302. Finally, we acknowledge A. Szabo and K. Ogilvie for WIND magnetic field and plasma data.

References

- Angelopoulos, V., The THEMIS mission, *Space Sci. Rev.*, *141*, 5–34, doi:10.1007/s11214-008-9336-1, 2008.
- Auster, H. U., et al., The THEMIS fluxgate magnetometer, *Space Sci. Rev.*, *141*, 235–264, doi:10.1007/s11214-008-9365-9, 2008.
- Burgess, D., On the effect of a tangential discontinuity on ions specularly reflected at an oblique shock, *J. Geophys. Res.*, *94*, 472–478, doi:10.1029/JA094iA01p00472, 1989.
- Eastwood, J. P., E. A. Lucek, C. Mazelle, K. Meziane, Y. Narita, J. Pickett, and R. A. Treumann, The foreshock, *Space Science Reviews*, *118*, 41–94, doi:10.1007/s11214-005-3824-3, 2005.
- Eastwood, J. P., S. J. Schwartz, T. S. Horbury, C. M. Carr, K.-H. Glassmeier, I. Richter, C. Koenders, F. Plaschke, and J. A. Wild, Transient Pc3 wave activity generated by a hot flow anomaly: Cluster, Rosetta, and ground-based observations, *J. Geophys. Res.*, *116*, A08,224, doi:10.1029/2011JA016467, 2011.

- Eastwood, J. P., et al., THEMIS observations of a hot flow anomaly: solar wind, magnetosheath, and ground-based measurements, *Geophys. Res. Lett.*, *35*, L17S03, doi:10.1029/2008GL033475, 2008.
- Fairfield, D. H., W. Baumjohann, G. Paschmann, H. Lühr, and D. G. Sibeck, Upstream pressure variations associated with the bow shock and their effects on the magnetosphere, *J. Geophys. Res.*, *95*, 3773–3786, doi:10.1029/JA095iA04p03773, 1990.
- Farris, M. H., and C. T. Russell, Determining the standoff distance of the bow shock: Mach number dependence and use of models, *J. Geophys. Res.*, *99*, 17,681–17,689, doi:10.1029/94JA01020, 1994.
- Farris, M. H., S. M. Petrinec, and C. T. Russell, The thickness of the magnetosheath: Constraints on the polytropic index, *Geophys. Res. Lett.*, *18*, 1821–1824, doi:10.1029/91GL02090, 1991.
- Fuselier, S. A., M. F. Thomsen, J. T. Gosling, S. J. Bame, C. T. Russell, and M. M. Mellott, Fast shocks at the edges of hot diamagnetic cavities upstream from the Earth’s bow shock, *J. Geophys. Res.*, *92*, 3187–3194, doi:10.1029/JA092iA04p03187, 1987.
- Glassmeier, K.-H., et al., Magnetospheric quasi-static response to the dynamic magnetosheath: A THEMIS case study, *Geophys. Res. Lett.*, *35*, L17S01, doi:10.1029/2008GL033469, 2008.
- Hartinger, M. D., D. L. Turner, F. Plaschke, V. Angelopoulos, and H. Singer, The role of transient ion foreshock phenomena in driving Pc5 ULF wave activity, *J. Geophys. Res.*, *118*, 299–312, doi:10.1029/2012JA018349, 2013.
- Horbury, T. S., D. Burgess, M. Fränz, and C. J. Owen, Three spacecraft observations of solar wind discontinuities, *Geophys. Res. Lett.*, *28*, 677–680, doi:10.1029/2000GL000121,

2001.

Jacobsen, K. S., et al., THEMIS observations of extreme magnetopause motion caused by a hot flow anomaly, *J. Geophys. Res.*, *114*, A08,210, doi:10.1029/2008JA013873, 2009.

Knetter, T., F. M. Neubauer, T. Horbury, and A. Balogh, Four-point discontinuity observations using Cluster magnetic field data: A statistical survey, *J. Geophys. Res.*, *109*, A06,102, doi:doi:10.1029/2003JA010099, 2004.

Le, G., C. T. Russell, M. F. Thomsen, and J. T. Gosling, Observations of a new class of upstream waves with periods near 3 seconds, *J. Geophys. Res.*, *97*, 2917–2925, doi:10.1029/91JA02707, 1992.

Lepping, R. P., et al., The WIND magnetic field investigation, *Space Sci. Rev.*, *71*, 207–229, doi:10.1007/BF00751330, 1995.

Lin, Y., Global hybrid simulation of hot flow anomalies near the bow shock and in the magnetosheath, *Planet. Space Sci.*, *50*, 577–591, doi:10.1016/S0032-0633(02)00037-5, 2002.

Lucek, E. A., T. S. Horbury, A. Balogh, I. Dandouras, and H. Rème, Cluster observations of hot flow anomalies, *J. Geophys. Res.*, *109*, A06,207, doi:10.1029/2003JA010016, 2004.

Maynard, N. C., W. J. Burke, D. M. Ober, C. J. Farrugia, H. Kucharek, M. Lester, F. S. Mozer, C. T. Russell, and K. D. Siebert, Interaction of the bow shock with a tangential discontinuity and solar wind density decrease: Observations of predicted fast mode waves and magnetosheath merging, *J. Geophys. Res.*, *112*, A12,219, doi:10.1029/2007JA012293, 2007.

McFadden, J. P., C. W. Carlson, D. Larson, M. Ludlam, R. Abiad, B. Elliott, P. Turin, M. Marckwordt, and V. Angelopoulos, The THEMIS ESA plasma instrument and in-

- flight calibration, *Space Sci. Rev.*, *141*, 277–302, doi:10.1007/s11214-008-9440-2, 2008a.
- Omidi, N., and D. G. Sibeck, Formation of hot flow anomalies and solitary shocks, *J. Geophys. Res.*, *112*, A01,203, doi:10.1029/2006JA011663, 2007.
- Omidi, N., J. P. Eastwood, and D. G. Sibeck, Foreshock bubbles and their global magnetospheric impacts, *J. Geophys. Res.*, *115*, A06,204, doi:10.1029/2009JA014828, 2010.
- Omidi, N., H. Zhang, D. Sibeck, and D. Turner, Spontaneous hot flow anomalies at quasi-parallel shocks: 2. Hybrid simulations, *J. Geophys. Res.*, *118*, 173–180, doi:10.1029/2012JA018099, 2013a.
- Omidi, N., D. G. Sibeck, X. Blanco-Cano, R.-C. D., D. L. Turner, H. Zhang, and Kajdič, Dynamics of the foreshock compressional boundary and its connection to foreshock cavities, *J. Geophys. Res.*, *118*, 823–831, doi:10.1002/jgra.50146, 2013b.
- Paschmann, G., G. Haerendel, N. Sckopke, E. Möbius, H. Lühr, and C. W. Carlson, Three-dimensional plasma structures with anomalous flow directions near the earth’s bow shock, *J. Geophys. Res.*, *93*(A10), 11,279–11,294, doi:10.1029/JA093iA10p11279, 1988.
- Plaschke, F., et al., Statistical study of the magnetopause motion: First results from THEMIS, *J. Geophys. Res.*, *114*, A00C10, doi:10.1029/2008JA013423, 2009.
- Potemra, T. A., H. Lühr, L. J. Zanetti, K. Takahashi, R. E. Erlandson, G. T. Marklund, L. P. Block, L. G. Blomberg, and R. P. Lepping, Multisatellite and ground-based observations of transient ULF waves, *J. Geophys. Res.*, *94*, 2543–2554, doi:10.1029/JA094iA03p02543, 1989.
- Schwartz, S. J., *Analysis Methods for Multi-Spacecraft Data*, chap. Shock and discontinuity normals, Mach numbers, and related parameters, pp. 249–270, ISSI Scientific Reports

SR-001, ESA Publications Division, 1998.

- Schwartz, S. J., R. L. Kessel, C. C. Brown, L. J. C. Woolliscroft, M. W. Dunlop, C. J. Farrugia, and D. S. Hall, Active current sheets near the earth's bow shock, *J. Geophys. Res.*, *93*(A10), 11,295–11,310, doi:10.1029/JA093iA10p11295, 1988.
- Schwartz, S. J., G. Paschmann, N. Sckopke, T. M. Bauer, M. Dunlop, A. N. Fazakerley, and M. F. Thomsen, Conditions for the formation of hot flow anomalies at Earth's bow shock, *J. Geophys. Res.*, *105*, 12,639–12,650, doi:10.1029/1999JA000320, 2000.
- Schwartz, S. J., D. Sibeck, M. Wilber, K. Meziane, and T. S. Horbury, Kinetic aspects of foreshock cavities, *Geophys. Res. Lett.*, *33*, L12,103, doi:10.1029/2005GL025612, 2006.
- Schwartz, S. J., et al., An active current sheet in the solar wind, *Nature*, *318*, 269–271, doi:10.1038/318269a0, 1985.
- Shue, J.-H., J.-K. Chao, P. Song, J. P. McFadden, A. Suvarova, V. Angelopoulos, K. H. Glassmeier, and F. Plaschke, Anomalous magnetosheath flows and distorted subsolar magnetopause for radial interplanetary magnetic fields, *Geophys. Res. Lett.*, *36*, L18,112, doi:10.1029/2009GL039842, 2009.
- Shue, J.-H., et al., Magnetopause location under extreme solar wind conditions, *J. Geophys. Res.*, *103*, 17,691–17,700, doi:10.1029/98JA01103, 1998.
- Sibeck, D. G., T. D. Phan, R. P. Lin, R. P. Lepping, and A. Szabo, Wind observations of foreshock cavities: A case study, *J. Geophys. Res.*, *107*, SMP 4–1 – SMP 4–10, doi:10.1029/2001JA007539, 2002.
- Sibeck, D. G., et al., Comprehensive study of the magnetospheric response to a hot flow anomaly, *J. Geophys. Res.*, *104*, 4577–4593, doi:10.1029/1998JA900021, 1999.

- Sonnerup, B. U. O., and M. Scheible, *Analysis Methods for Multi-Spacecraft Data*, chap. Minimum and maximum variance analysis, pp. 185–220, ESA Publications Division, 1998.
- Thomas, V. A., D. Winske, M. F. Thomsen, and T. G. Onsager, Hybrid simulation of the formation of a hot flow anomaly, *J. Geophys. Res.*, *96*, 11,625–11,632, doi:10.1029/91JA01092, 1991.
- Thomsen, M. F., J. T. Gosling, S. J. Bame, K. B. Quest, C. T. Russell, and S. A. Fuselier, On the origin of hot diamagnetic cavities near the earth’s bow shock, *J. Geophys. Res.*, *93*(A10), 11,311–11,325, doi:10.1029/JA093iA10p11311, 1988.
- Turner, D. L., S. Eriksson, T. D. Phan, V. Angelopoulos, W. Tu, W. Liu, W. L. Teh, J. P. McFadden, and K. H. Glassmeier, Multispacecraft observations of a foreshock-induced magnetopause disturbance exhibiting distinct plasma flows and an intense density compression, *J. Geophys. Res.*, *116*, A04,230, doi:10.1029/2010JA015668, 2011.
- Turner, D. L., N. Omidi, D. G. Sibeck, and V. Angelopoulos, First observations of foreshock bubbles upstream of Earth’s bow shock: Characteristics and comparisons to HFAs, *J. Geophys. Res.*, *118*, 1552–1570, doi:10.1002/jgra.50198, 2013.
- Völk, H. J., and R.-D. Auer, Motions of the bow shock induced by interplanetary disturbances, *J. Geophys. Res.*, *79*, 40–48, doi:10.1029/JA079i001p00040, 1974.
- Wang, S., Q. Zong, and H. Zhang, Cluster observations of hot flow anomalies with large flow deflections: 1. velocity deflections, *J. Geophys. Res.*, *118*, 732–743, doi:10.1002/jgra.50100, 2013a.
- Wang, S., Q. Zong, and H. Zhang, Cluster observations of hot flow anomalies with large flow deflections: 2. bow shock geometry at HFA edges, *J. Geophys. Res.*, *118*, 418–433,

doi:10.1029/2012JA018204, 2013b.

- Wu, B. H., M. E. Mandt, L. C. Lee, and J. K. Chao, Magnetospheric response to solar wind dynamic pressure variations: Interaction of interplanetary tangential discontinuities with the bow shock, *J. Geophys. Res.*, *98*, 21,297–21,311, doi:10.1029/93JA01013, 1993.
- Zhang, H., D. G. Sibeck, Q.-G. Zong, S. P. Gary, J. P. McFadden, D. Larson, K.-H. Glassmeier, and V. Angelopoulos, Time History of Events and Macroscale Interactions during Substorms observations of a series of hot flow anomaly events, *J. Geophys. Res.*, *115*, A12,235, doi:10.1029/2009JA015180, 2010.
- Zhang, H., D. G. Sibeck, Q.-G. Zong, N. Omid, D. Turner, and L. B. N. Clausen, Spontaneous hot flow anomalies at quasi-parallel shocks: 1. Observations, *J. Geophys. Res.*, *3357-3363*, 3357–3363, doi:10.1002/jgra.50376, 2013.

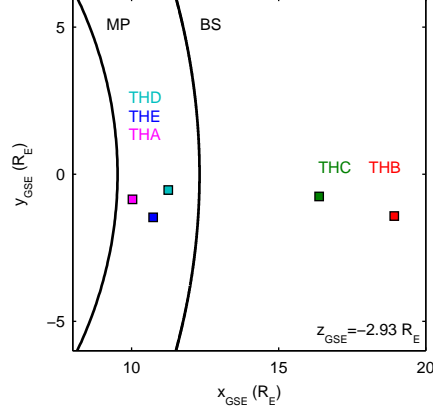


Figure 1: Positions of the five THEMIS spacecraft in GSE on 04 September 2008 at 17:32-42 UT. The *Shue et al.* [1998] model magnetopause (MP) and the *Farris et al.* [1991] model bow shock (BS) with standoff distance set by *Farris and Russell* [1994] are also shown.

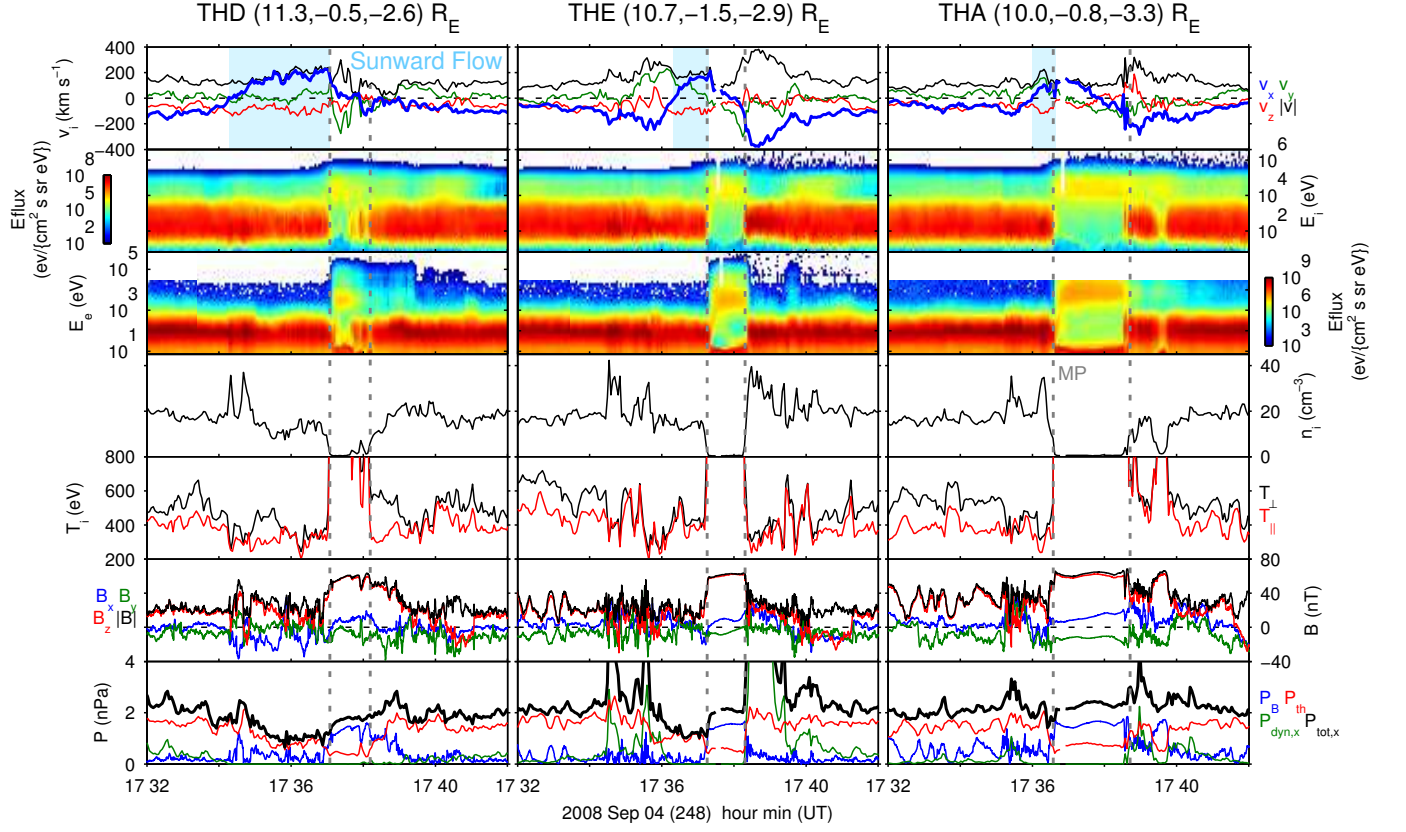


Figure 2: Magnetosheath observations from THD (left), THE (middle) and THA (right). From top to bottom: the ion velocity components in GSE (x, y, z in blue, green, red) and magnitude (black); ion energy spectrogram where the colour scale represents the differential energy flux; electron energy spectrogram; ion density; ion temperatures parallel (red) and perpendicular (black) to the magnetic field; magnetic field components in GSE (x, y, z in blue, green, red) and magnitude (black); and the magnetic (blue), thermal (red), anti-sunward dynamic (green) and total anti-sunward (black) pressures. Plasma and magnetic field data are shown at resolutions of 3 s and 0.25 s respectively. The blue shaded regions indicate magnetosheath flows with a sunward component and vertical grey dashed lines highlight magnetopause crossings.

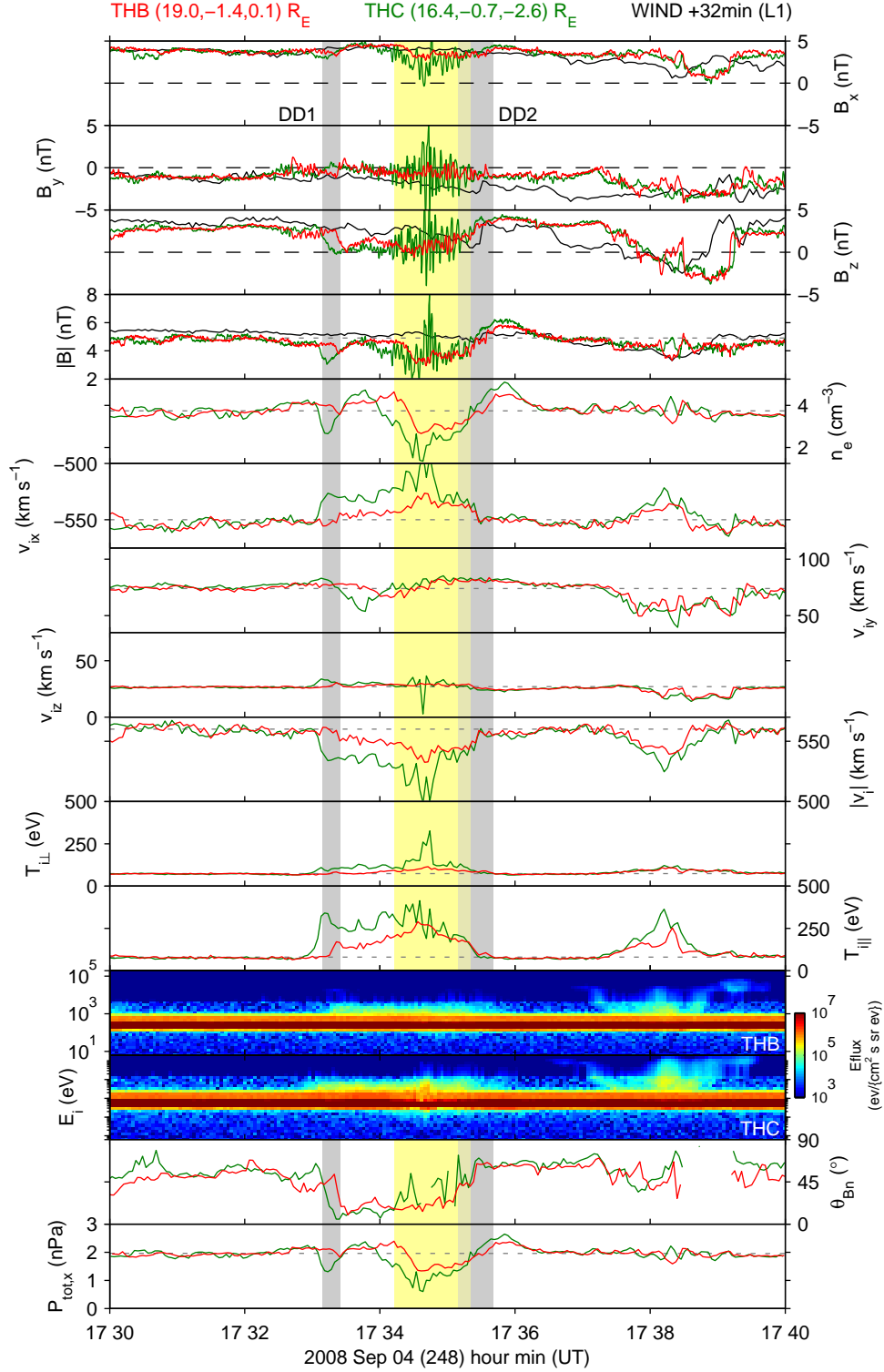


Figure 3: Solar wind/foreshock observations from THB (red), THC (green) and WIND (black), with the latter lagged by 32 min. From top to bottom: x,y & z components of the magnetic field in GSE; magnetic field strength; electron density; x,y & z components of the ion velocity in GSE; magnitude of the ion velocity; ion temperatures perpendicular and parallel to the magnetic field; ion energy spectrograms; electron energy spectrograms; magnetic field - shock normal angle θ_{Bn} magnetically connected to the spacecraft; and the total anti-sunward pressure. Plasma and magnetic field data are shown at resolutions of 3 s and 0.25 s respectively, while θ_{Bn} is calculated using 3 s resolution magnetic field data. Shaded areas highlight two directional discontinuities (DD1 & DD2) in grey and a region of depleted density and magnetic field in yellow.

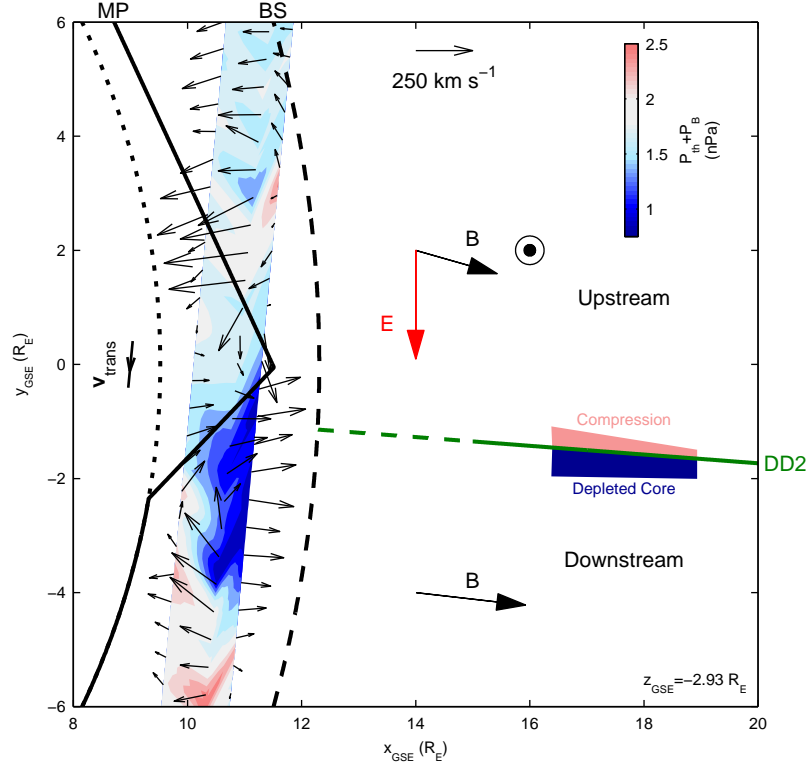


Figure 4: Snapshot of the event at 17:37:00 UT in the x-y GSE frame. The observed magnetopause (MP) deformation (solid black) combined with the *Shue et al.* [1998] model (dotted black), the *Farris et al.* [1991] model bow shock (BS, dashed black) and the current sheet DD2 (green) are shown. The IMF and motional electric field either side of DD2 are given by the black and red arrows respectively (note that on the downstream side the electric field is negligible due to the radial IMF). We display the observed flow pattern (black arrows), the transit speed \mathbf{v}_{trans} of the magnetopause bulge, and contours of the thermal + magnetic pressure (colour scale). The observed depleted core and compression regions of the transient are indicated either side of DD2, with colours representative of the total pressure in each.